

4) Assessment of the degree of spin-phonon, spin-spin dynamics in the synthesized compounds.

Chapter 2. Equipment and measurement technique.

§ 2.1. Receiver sensitivity sensor NQR and conditions optimum adaptation to the measuring chamber.

As is known, the sensitivity of the receiving path to radio spectrometer NQR absorption signals defined set of parameters [27]. Thus, according to the survey [64], S / N ratio of the signal to noise ratio at the receiver output can be represented as:

$$S/N = \frac{\alpha N Q \xi r^2}{\sqrt{4k_B) Q N^2 \nu_0 T_r \sqrt{r + R_{ecv} T_{ecv}}} \quad (2.1)$$

where α - nuclear spin contribution, N and r - the number of turns and the radius of the solenoid, Q - Q-factor of the receiver coil, B - receiver bandwidth, T_c - temperature of the resonator, ξ - the filling factor of the resonator, $R_{eq} T_{eq}$ - equivalent resistance and temperature receiver, ν_0 - quadrupole resonance frequency.

In this section we will carry out examination of the conditions that must be considered when designing NQR cameras to increase the quality factor of the receiving circuit. As is known, this value is limited by the condition $Q < 1,5 \nu_0 \tau_{im}$ where τ_{im} - lifetime free induction signal. In NQR typically $Q < 150$. However, the location of the sensor in the NQR shell, which is a body of a device external influence on the sample, the Q value is significantly reduced due impedansnoy sensor communication with the shell of the device. This relationship can be expressed as follows [65]:

$$Q = \frac{\nu W}{P} \quad (2.2)$$

where W - energy stored in the resonator, P - power loss associated in particular with the dissipation of energy in the environment of the resonator. To calculate the losses it is necessary to estimate the energy W . As we know the energy of interaction between two conductors is expressed through the inductive factor L_{12}

$$W_p = \frac{1}{8\pi} \oint \vec{H} \circ \vec{B} \circ dV : \frac{L_{12} J_1 J_2}{C^2} \quad (2.3)$$

where J - volume currents. In case the interaction of the solenoid (radius r and length $l(1)$) with a cylindrical shell (radius R , the length L and the thickness H) according to [66] has an analytical expression:

$$L_{1/2} = \int_{k-1}^N \int_{0-1/2}^0 \frac{r(R+H/2) \cos \phi d\phi dL}{\sqrt{\frac{aL-1+1/N}{c} - k \frac{1}{N} \frac{\ddot{\phi}}{\phi} + \frac{a}{c} R + \frac{H}{2} \frac{\ddot{\phi}}{\phi} + r^2 + 2 \frac{a}{c} R + \frac{H}{2} \frac{\ddot{\phi}}{\phi} r \cos \phi}} \quad (2.4)$$

where N - number of coil turns, φ - polar angle. Integral in the general case is calculated numerically, but $L \rightarrow \infty$ is expressed in terms of elliptic functions. In the frequency range ($\omega R < c$) can be obtained for the magnitude P loss following expression [65]:

$$\frac{W}{t} = P : \frac{\pi^2 \mu^2 \omega J_0^2}{\sqrt{\sigma} \epsilon c^2} + \dots \quad (R > r) \quad (2.5)$$

where (μ and σ - magnetic permeability and conductivity of the shell, and take into account the higher-order bias currents, giving an increasing contribution at $\omega R = c$.

Knowing the energy of a cylindrical solenoid [65]

$$W = \frac{2\pi r^2 n I^2 \mu}{c^2 \epsilon} - \frac{8r}{3\pi l} + \dots \quad (2.6)$$

we can evaluate how the cavity Q depends on some dimensional parameters:

$$Q : \frac{2l\sqrt{\sigma}}{\pi r^2 \mu \omega^2 \epsilon} - \frac{8r}{3\pi l} + \dots \quad (\text{With } R > r) \quad (2.7)$$

For high frequencies (in this case more than 10^8 Hz) observed other addiction [66, 67].

The estimates show, in particular, that the Q value decreases with the increase of the radius r of the solenoid proportional to its square. Midrange in losses will contribute as part of the capacitive impedance of the system.

Returning to the value of the ratio of school, we can see that from the point of view of the geometry of the coil placed in the shell, school increases with the radius and the length of $S/N \approx r\sqrt{l}$. However, the length of the L shell in the real world is always limited and decreasing $L - l(1)$ will increase energy leakage near the ends of the solenoid [67]. Therefore, we can assume that when choosing some optimal geometric relationships between the dimensions of the shell and coil, SN ratio can be increased by increasing the radius of the coil. Expression (2.7) is rather illustrative indication to select geometry and material characteristics of external consoles NQR. In our case, this is due to the fact that a large part of the diapason of frequencies used, is in a quasi-stationary region field ($\omega R \approx c$) (the mids). Therefore, prior to making the designs consoles external influence, we chose the optimal geometry by measuring the quality factor resonators NQR directly on layouts and finished products.

It was established experimentally that SN ratio increases with increasing radius of the receiver of the NQR sensor up to a value which is approximately half the size of the internal outer shell. The magnitude of the energy loss depends on the magnetic and conductive properties of materials. As shown in [68] and it follows from (2.5), a conductive shell for high frequency loss value decreases with increasing the conductivity of the shell. In the case of dielectric shells made loss due to the bias currents, and increase with frequency. The magnitude of dielectric loss is essentially independent of the geometry of the shell.

These principles have been taken into account in the design world and improve termoprstavok NQR for research and used in the development and manufacture of high-pressure chamber with increased sensitivity to signals NQR (see § 2.2 and 2.4).

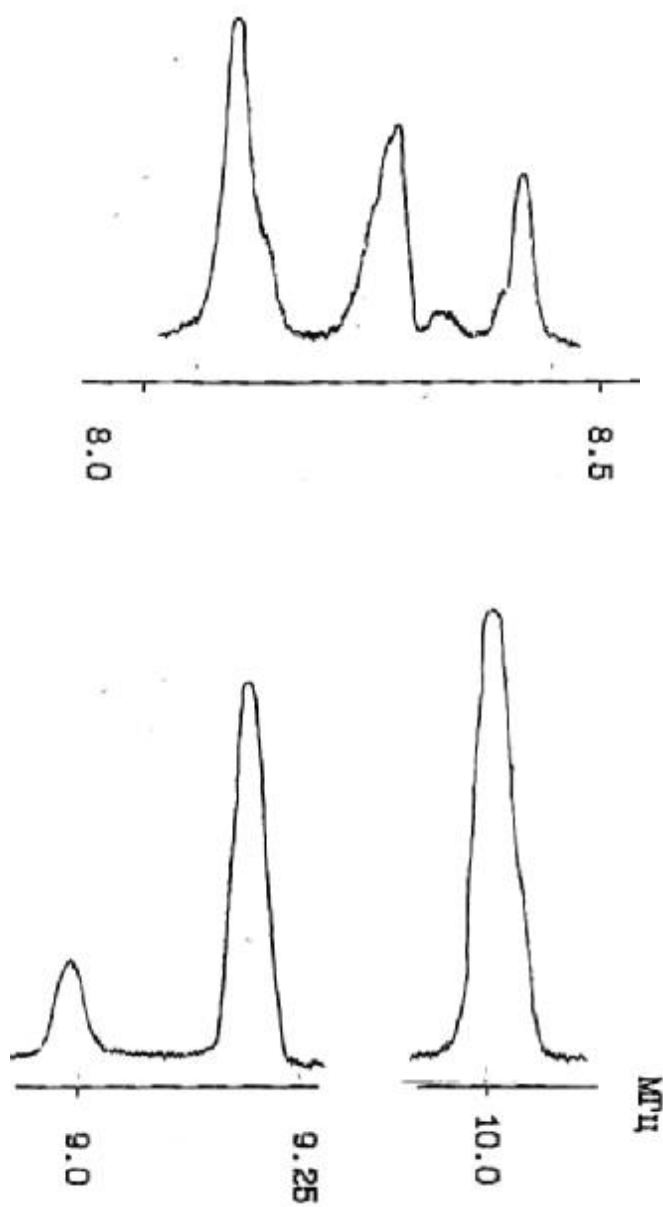


Figure 2.1. NQR spectrum ^{35}Cl in K_2ZnCl_4 at room temperature

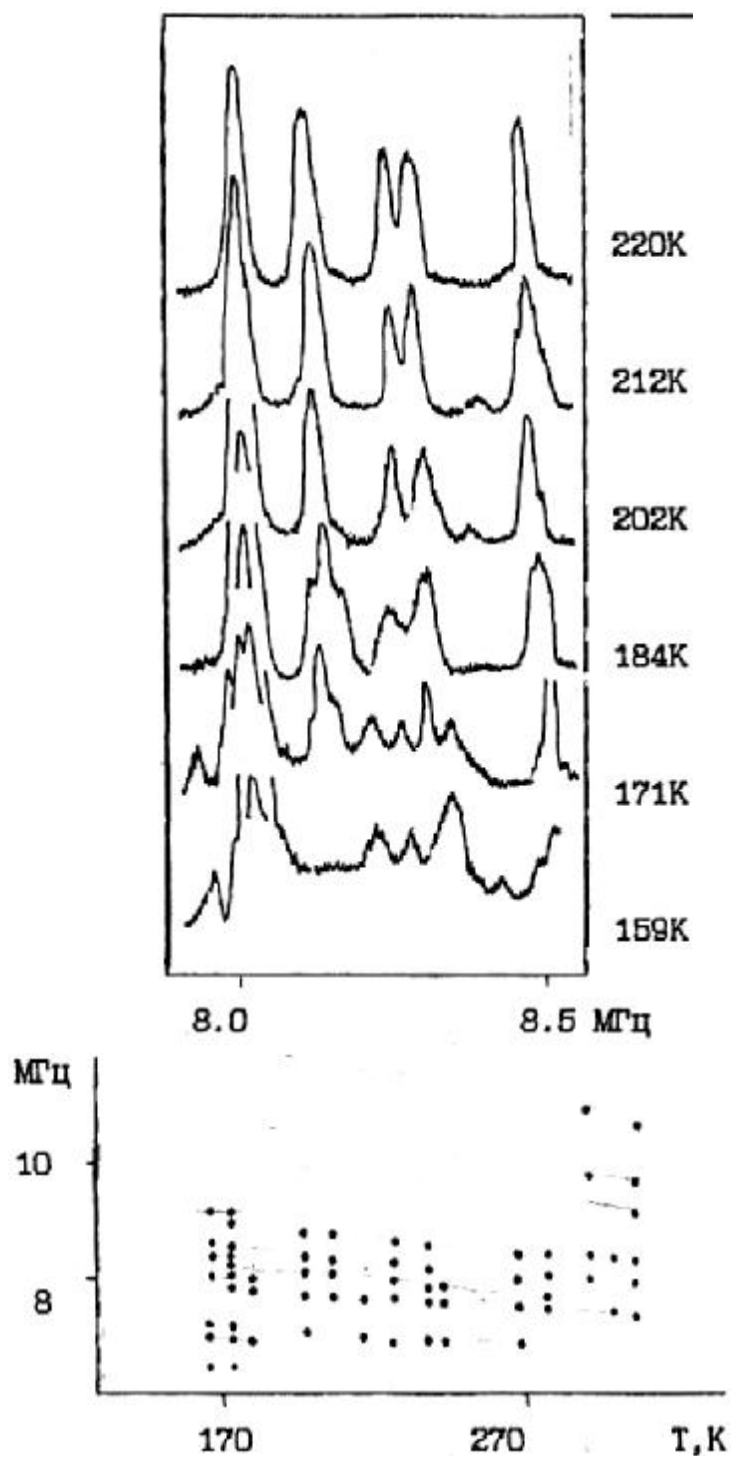


Figure 2.2. The temperature dependence of NQR spectrum and in K_2ZnCl_4 in the range of 8-8.5 MHz.

Originally optimal matching method (OM) was tested at check NQR signals from nucleus ^{37}Cl and ^{35}Cl compound K_2ZnCl_4 with a structure of $\beta\text{-K}_2\text{SO}_4$. This compound was initially investigated by the NQR spectrometer superregenerativnogo type in a chemistry lab minerals Klaytona city, Australia, Scaife [44]. At ambient temperature was revealed six signals from nucleus ^{35}Cl , in the frequency domain with 8-10MHz ratio S/N = 6--12 units. At liquid nitrogen temperature signals are absent. Later, at the Institute of Materials Attica, NQR in K_2ZnCl_4 found three phase transition at $T_i = 553\text{K}$, $T_{C1} = 403\text{K}$ and $T_{C2} = 145\text{K}$ [37]. When this was recorded only part of the full spectrum of ^{35}Cl NQR near 560K and below 290K. Signal to noise ratio was in the range 0—12 units. The first attempt to study this connection, we noted only weak NQR signals at liquid nitrogen. Application of the method allowed us to fix the OS full NQR spectrum (Figure 2.1) at room temperature (RT). S/N ratio was 10--25 units. In the frequency range 8,5-8,0 MHz NQR observed spectral lines are not marked in [37]. Fig. 2.2 shows the temperature variation of the NQR spectrum of K_2ZnCl_4 and the temperature dependence of the frequency $\nu(T)$. For high-frequency part of the spectrum at $T = 290\text{K}$, unlike us Milian observed broadened singlet absorption line NQR. At $T = 173\text{K}$ observed anomaly associated with the redistribution of intensities and frequencies of the spectrum. Simultaneously with our measurements, different researchers using mutually complementary methods observed phase transition in this temperature range [69,70]. However, some significant variations in the temperature of this transition and reusability of data. As explained later, it was the result of significant non-equilibrium processes characteristic of this class of compounds I.

§ 2.2 The temperature set-top spectrometer for studying phase transitions.

Standard termopristavka ISS (ИЦИИ) spectrometer series, the fan with the principle of mixing the gaseous medium to equalize the temperature gradient on the sample did not meet the requirements of our traditional measurements. Its disadvantage is a) a high temperature gradient to 3 K/sm; b) a great time for temperature stabilization.

The design of the heat chamber, where the heat setting is performed by blowing coolant opposite directions two-way screw channels, Rout in the copper shell, also had drawbacks, the main one of which is a large factor of the inductive-capacitive sensor relationship with NQR.

To achieve the objectives of our research the author has developed and tested new thermal cameras. Figure 2.3 shows liquid heat chamber for research NQR. The basic idea inherent in the design of the thermal cameras, is the replacement of the gas on the liquid medium, providing better heat transfer properties. The main difference lies in the design hermetically sealed housing (3) place the sample location and input axis (4a) of the fan and removing conductive material from the NQR sensor (2). For this inner housing chamber (1) was made of PTFE with a sealing compound in removable input coils NQR. Liquid completely fills the entire volume of the chamber. Small evaporation silnoletuchih replenishes fluids communicating through PTFE hose (6) to maintain the system level. Temperature sensor (5) housed in a shielded casing away from the sample. At the bottom there was a heat chamber shielded stove (7), which was used in the auxiliary heating. The

whole system was placed in a standard Dewar flask, made in the form of two communicating vessels. Changing the temperature and maintaining the nitrogen purge was

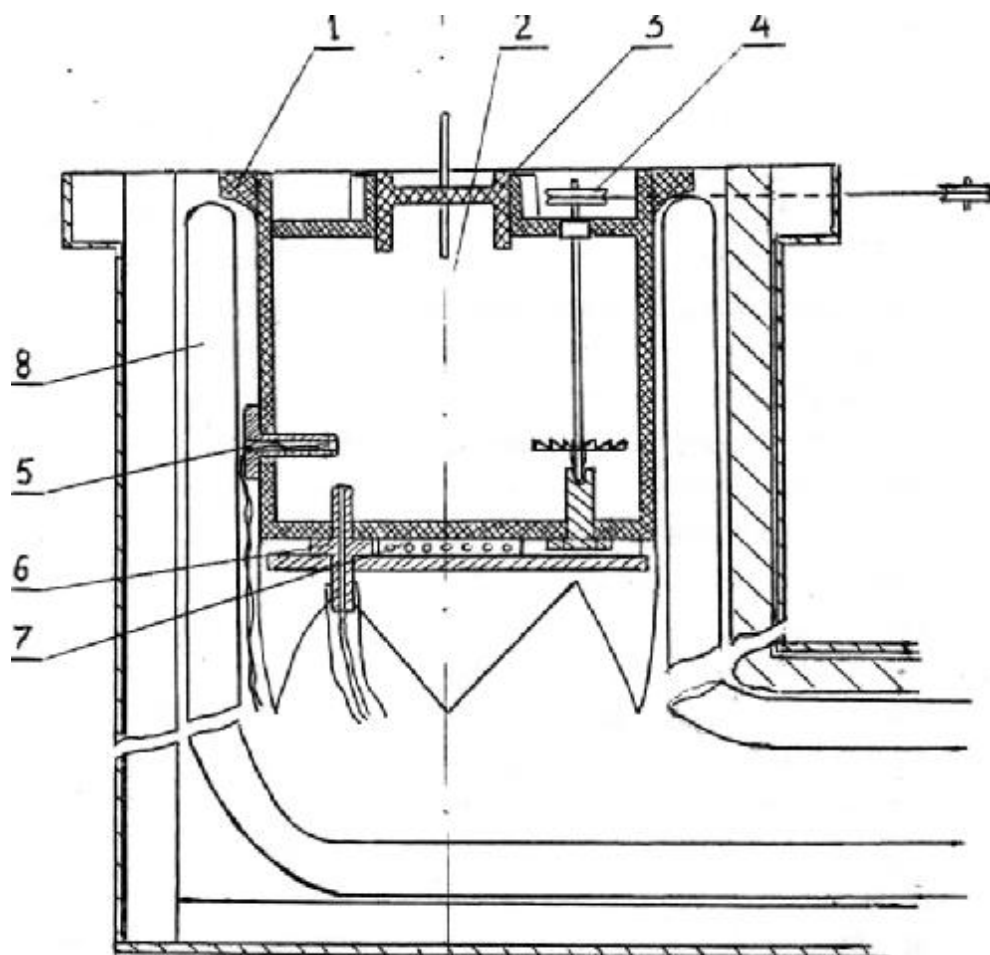


Figure 2.3. Liquid-gradient heat chamber for NQR Science.
1. The body; 2. NQR sensor; 3. Seal sensor; 4. The agitator; 5. termopara; 6. Platinum thermometer; 7. Heater; 8. Dewar.

carried out through a tube connected to the second portion dewar. As the refrigerants used n-pentane (liquid state region $138 < T < 320\text{K}$) hexane, transformer, silicone oils, glycerol ($T = 600\text{K}$), and other inert liquid sample. The temperature gradient in the zone of the sample out (to 0.01 K/cm).

The disadvantage is the need to change the thermal cameras or olive liquid (which could be carried out during the measurements) in different temperature ranges. At temperatures below 140K (the crystallization point of pentane), its characteristics are deteriorated. To overcome these drawbacks, chamber design required improvements. The result has been designed, tested and used in the study of phase transitions in Cs_2ZnJ_4 and $(\text{NH}_4)_2\text{ZnJ}_4$ heat chamber shown in Figure 2.4. Its features is the use of an external circulation mode gas purge. In the first case the fluid circulates in the plane of the heat chamber (1) in the upper part of the conjugate through the sealing compound (d) directly to a bayonet flange gasket spectrometer (3). In the case of a gas purge gas (mixture) is blown through the lattice (4) promoting samoperemeshivaniyu hydrodynamic flows. Temperature range when running in automatic mode, determined by the characteristics of the circulation thermostat (for U-16 is $210\text{K} - 400\text{K}$). Outside this range, additional stabilization of the temperature applied. The temperature gradient in the region of the sample out. Time alignment when the temperature gradient was from 2 to 10 minutes. In the gradient mode, the gas temperature at the sample was $0.1-0.2 \text{ /sm}$.

Minimum distance sensor NQR spectrometer to releasably nest and exclusion metallic structural elements described in thermo-console NQR allowed to achieve maximum inductive capacitive matching inductor NQR with alarm transmission paths ISSH spectrometer. Using the receiver coils with an increased (compared with standard) diameter (20 mm) allowed to increase the signal-to-noise ratio (S/N) 5-8 times.

§ 2.3 Synthesis of samples.

Most of the compounds A_2BX_4 used in our experiments, was grown in the laboratory of the Institute of Physics of crystals. L.V.Kirenskogo AS RU. From aqueous solutions of crystals grown V.A.Grankinoy. Bridzhmen method of melt compounds synthesized to I.T.Kokov. Connection Cs_2ZnJ_4 , $(\text{NH}_4)_2\text{ZnJ}_4$ and others for NQR studies were synthesized by the author.

During crystallization from solution, the deviation from the stoichiometric ratio of the starting chemical components AX and BX_2 was chosen empirically, taking into account their degree of hydration. The composition of the samples was identified based on the reference [71] and periodic data [72, 73, etc.].

Connection of A_2BX_4 (K_2ZnCl_4 , Rb_2ZnBr_4 , Cs_2ZnJ_4 , Cs_2CdJ_4 , $(\text{NH}_4)_2\text{ZnJ}_4$) usually crystallized in the form of single-crystal plate splices up to 40mm and a thickness of 5mm . Were synthesized as large single crystals. compounds of other compositions (A_2BX_5 , ABX_3 , etc.) have had other forms of habit. Some samples of A_2BX_4 to remove impurities, subjected to repeated recrystallization (Rb_2ZnBr_4 , Cs_2ZnJ_4). Polycrystalline, blocky or monobloc crystals (Cs_2CdJ_4 , $(\text{NH}_4)_2\text{ZnJ}_4$) were prepared from the melt.

Due to the difficulties in carrying out the exact chemical analysis (which was carried out with precision 2%. only for Rb_2ZnBr_4), the degree of purity of samples was evaluated by

the criteria proposed by Hamano [52,72]. According to the cited studies, the magnitude of the concentration of impurities in the compounds Rb_2ZnCl_4 and Rb_2ZnBr_4 , significantly

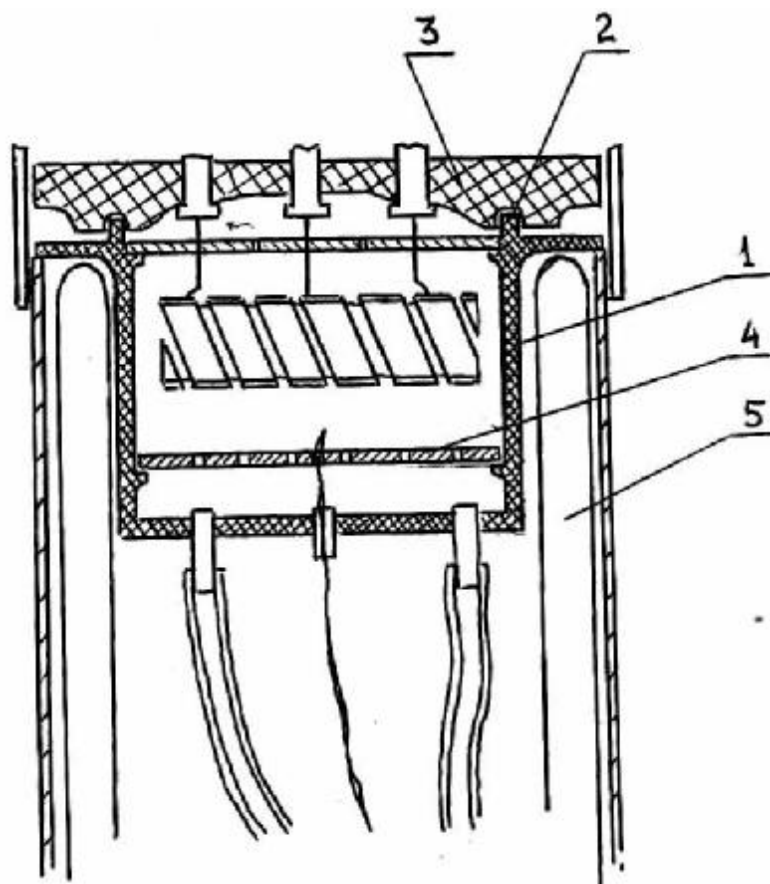


Figure 2.4. Gas-liquid heat chamber NQR :. 1. The body; 2. Sealing compound; 3. Flange spectrometer; 4. Grille; 5. Thermal insulation casing; 6. Thermocouple.

affects the amount of thermal hysteresis of the phase transition at T_C ferroelectric phase, as well as on-time behavior quadrupole spin-lattice relaxation time T_{1Q} . For undoped samples hysteresis decreases significantly and there is racing. For example, for the compound $\text{Ba}_2\text{CoGe}_2\text{O}_{10}$, where in hysteresis phenomena are significantly dependent on the concentration of impurities, the amount of thermal hysteresis $\Delta T = T_C^c - T_C^h$ samples from various stages of crystallization in this case was 8 -- 3 K.

An additional criterion was the degree of purity of the NQR spectral linewidth in the ordered phase. For the most thoroughly homogeneous width of the synthesized compounds were single lines 100-90 kHz.

§ 2.4 Apparatus for NQR studies under high hydrostatic pressure.

Since 1972 year, the Institute of Physics L.V.Kirenskogo USSR Academy Krasnoyarsk Serebrennikov V.L. and Moskalev A.K., [74,75] developed a high-pressure apparatus applied to radiospectroscopic methods. Such equipment, including the need to study phase P-T diagrams of dielectric crystals. Particularly relevant is the use of this instrument for the study of disordered structures neglected, what are incommensurate phases. Detailed description of the devices and technology of high pressure is presented in the monograph [74]. In this section we present the basic principles of experimental and some technical details on which created a new and improved traditional experimental setup.

Typical complex laboratory equipment used in research of structural phase transitions in crystals NQR, including at high hydrostatic pressure is shown in Figure 2.5. It consists of the following components: 1) spectrometer NQR 2) changes in the system, control and maintain the temperature and pressure (SIKPD).

The main units SIKPD are high-pressure chamber (1), the multiplier (8), a pumping station (9), Electronic Stability and pressure measurement (10). High pressure (HPC) is in direct mechanical contact with flange-receiving slot of the spectrometer transmission unit in a heat-insulating and shock-proof housing. At its bottom, a bomb attached to a multiplier, in which the working chamber through the oil passages (12) from the pump station (9) Hydraulic oil is supplied. End transmits pressure to the piston first multiplier, and further through the piston is created pressure buildup in the medium surrounding the sample (as the medium used hydrostatic pentane mixture with the transformer oil.) The temperature and pressure of the liquid around the sample were measured respectively copper-constantan thermocouple and manganin gauges. Measurement and control of temperature and pressure using standard measuring circuit using potentiometers P309 and P363/Z and bridge resistors P39.

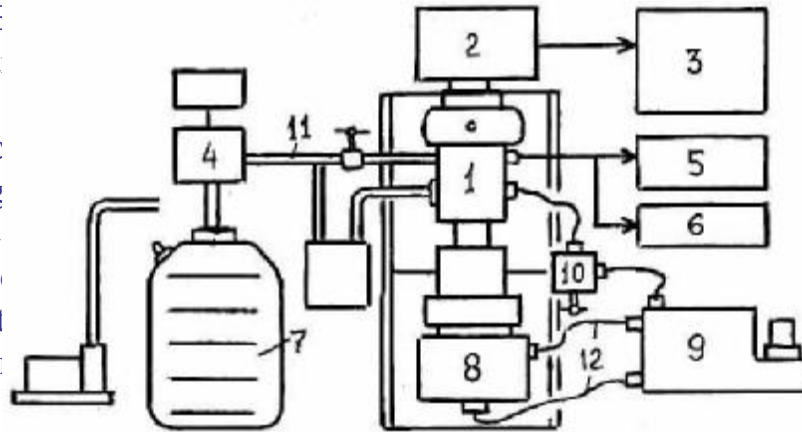
Thermal stabilization system consists of a cold finger (11), which passed the vapor stream of nitrogen, and the electronic device (4) with a system of heaters thermostabilizing elements of the system. At positive temperatures using liquid coolant, thermostabilizing circulator.

The study applied a few high pressure chambers. In the high-temperature measurements were carried out in a cell made of a titanium alloy BT-6C [74,75]. At low temperatures and used camera HPC1 HPC2 made of beryllium bronze (BrB2).

Chamber HPC1 designed to operate over a wide range of pressures (up to 1,5 GPa (= 1,5 Kbar)). Its design is presented in Figure 2.6. The camera body (1) has an outer

diameter of 80 mm. Inner through-channel (2) with a chamber diameter of 16 mm. At the transitions NQR at

Figure 2.5. High hydrostat



1. Pressure conductor
2. Receiving coil
3. NQR spectrometer
4. Electronic inputs
5. Temperature sensor
6. Pressure sensor
7. Dewar;
8. Multiplier
9. Pumping station;
10. Device stabilization system pressure;
11. Thermal inputs;
12. Oil - input.

top of the channel is the radio frequency coil NQR (3). Electrical inputs of coils are soldered to the bottom of the high-voltage electric inputs (4). Contact with the spectrometer unit provided top of the electric inputs. Recent resin-sealed channels ED-20 filler. One of the channels used for output

conductor pressure sensor and thermocouple. Coaxially receiving coil is a silver foil shield (5). Obturator with a set sealing bronze-copper-lead-rings (7) fixed bearing nut (8). The lower part of the HPC is installed on the multiplier. All parts of the camera heat treated to a hardness of 3540 units in the scale of HRC.

Usage tapered seal wiring impulse withstand voltage up to 2.5 kV at a pressure up to 10 kbar. Electric high capacity electric inputs was about 10 pF. Q factor specially manufactured receiver coils mounted in the chamber, was $Q = 12, 18$ units at 50 MHz. Range interface receiving and transmitting paths of the spectrometer is within the 5, 6 MHz.

In the operation of the high temperature compartment HPC1 been ascertained that the quality factor of the NQR sensors in these cells is not sufficient for detailed studies in the field of spectra disproportionate phases. In addition, the presence of significant inductive coupling sensors with camera body, significantly restricted range of frequency matching paths spectrometer, in connection with which tracked a narrow frequency range of spectra and worse accuracy. Another disadvantage is imperfect system input sensors for measuring P-T parameters. Siting in the vicinity of high-voltage electric wires caused additional deterioration of merit and immunity NQR sensor and on the other hand, increased the high-frequency and capacitive crosstalk on themselves P-T sensors. Small amount of volume of the pressure medium, a high value of the residual pressure (about 0.4 kbar) after decreasing from larger values create more difficulty in the experimental work in the field below 0.6 kbar. To address these shortcomings, and in accordance with the task was developed and produced a new high-pressure chamber HPC2.

The design is presented in Figure 2.7 HPC2. The camera body (1) (external diameter 80mm) has an inner diameter of 40mm working where and placed RF NQR sensor (2).

The channel (3) for movement of the piston (4) has an enlarged diameter 20mm. By implementing the new design of the obturator (5) has been reduced to three times the length of high voltage electrodes (6). Diameter electric inputs for channels has been increased to 2,5 mm. Connection and sealing shutter with the camera body is provided with special mounting clips (7) with the counter buttress thread. Used in this type of seal chamber is specially designed by us for large diameter channels and is based on the hydraulic chamber through the mating of the parts bronze ring of triangular section (8).

To enter P-T sensors using an additional seal (9) located on the side of the camera. It is attached to the snap ring (10). The same ring is used to attach the nuts (11) sealing the capillary nozzle (12) through which the hydraulic fluid pumping work and message of the working volume of the chamber through the valve with atmospheric pressure.

Shielding PT sensors from inductive capacitive coupling coil NQR is achieved by installing a thin-walled silvered screen The screen is also used to reduce the inductive capacitive coupling coil with the camera body. Heat exchange with the coolant used two copper jacket (14) with single-sided spiral groove.

Under this design were manufactured receiving sensors up to 22mm diameter. Sensors electric inputs and coated with a layer of silver of about 1 micron. Q factor coils mounted

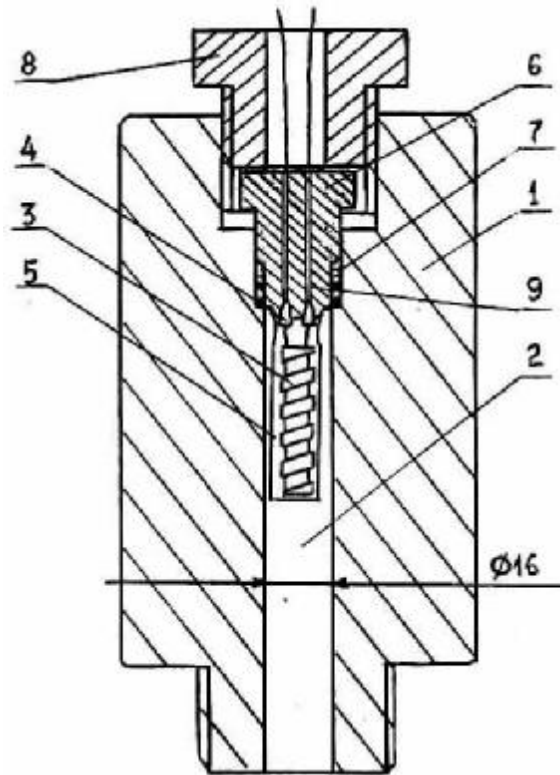


Figure 2.6. The design of high-pressure chamber (CHP1) for NQR study.

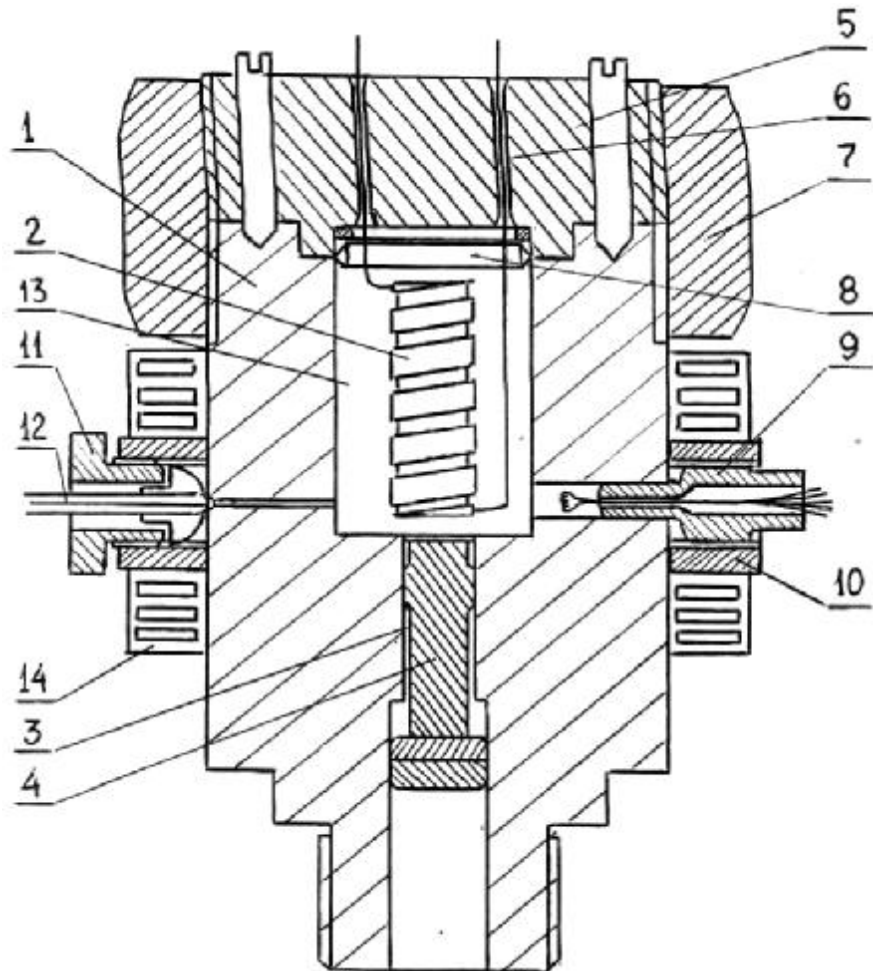


Figure 2.7. The design of high-pressure chamber (HPC2) with large inner diameter.

at 8, 10mm diameter - Q 80, 100 at diameters 20mm - Q » 60. The signal-to-noise ratio increased 4 times in HPC1.

Improved frequency-amplitude matching NQR sensors with alarm transmission paths spectrum. Used to 12 MHz, which, in particular, has allowed further simultaneously capture NQR spectrum of the nucleus in the structure of Rb_2ZnBr_4 .

Frequency measurement of the signal amplitude and the ratio S/N became comparable with its own standard cameras spectrometer (Table 2.1).

Comparison of errors changes in temperature, pressure, frequency, and the signal/noise ratio under different conditions.

Value units	T degree	bar	Frequency	Intensity	S/N for different frequencies	times
chamber	± 0.05	-	$0.5 \pm 0.02\%$	»5%	100, 10	10
		± 100	$1 \pm 3\%$	»50%	40, 0	
	± 0.5	± 10	$0.5 \pm 1\%$	25%, 15%	80, 0	
	± 1	± 200	$2 \pm 3\%$	»80%	20, 0	

High-pressure chamber (F
*)